Ion sputtering yield measurements for submicrometer thin films

Nina Veisfeld
Digital Equipment Corporation, Northboro, Massachusetts 01532
Joseph D. Geller
Geller Microanalytical Laboratory, Peabody, Massachusetts 01960

(Received 5 October 1987; accepted 9 November 1987)

Most of the published ion sputtering yield values are based on experimental techniques which do not correlate well with the ion sputtering process commonly used with surface analysis instrumentation. A need exists for ion sputtering yield measurements collected under the same conditions which will be used in practice. We have measured ion sputtering yields on several sputter-deposited metal films using the Auger electron spectroscopy "breakthrough" depth profile method, whereby characteristic Auger electron transitions for the thin film and the substrate are monitored while the thin film is being sputtered away. Rutherford backscattering spectrometry is used to measure the density of the films and a scanning stylus profilometer is used to measure the depth of the resulting sputter craters. The thin metal films exhibit a sputtering rate depth dependency, i.e., the sputtering decreases with the amount of material removed. It was shown that this phenomenon is related to surface roughening due to the directionality of the ion sputtering process. Reduction of the topographic effects with a significant improvement in depth resolution is demonstrated by continuously rotating the sample during ion bombardment.

I. INTRODUCTION

Auger electron spectroscopy combined with ion sputtering is a universally recognized analytical method which is commonly used to characterize thin films and interfaces for composition and diffusion. The films' behavior is critically dependent upon their deposition parameters and subsequent thermal or chemical treatments. Depth profiles are generated using the ion sputtering process to remove the surface layer of the analyzed material while Auger electron spectroscopy measurements determine the compositional changes through the depth of the analyzed material. The resulting data are normally plotted as atomic concentration versus sputtering time.[1] It is desirable instead to represent the composition as a function of depth. This task is formidable since the sputtering rate (usually described in Å/min or nm/min) requires knowledge of both the absolute sputtering yield (atoms/ion) and the density for each of the sputtered materials.

II. SPUTTERING YIELD CONSIDERATIONS

One must be prudent when selecting a sputtering yield reference value for determining the thickness of material removed during the sputtering process. Published sputtering yield values for various elements, mixtures, and compounds in amorphous, poly- and single-crystalline states of thin, thick, or bulk structures[2,3] exhibit significant variability, sometimes by several hundred percent, for the same material composition and sputtering beam ion species and energy. These discrepancies are attributed to variations in the composition and preparation of the materials analyzed and the experimental conditions under which the measurements have been made.

Sample related factors to consider are composition, topography, surface contamination, crystallographic structure, impurities, defects, and phase variations. Of these, the crystallographic structure of the specimen and its orientation to the sputtering ion beam may be the most significant. This will be considered in more detail later. For thin films, the deposition method (evaporation, sputtering, plating, etc.) and conditions under which the films were prepared (gas composition, deposition rates, field potentials, temperature, etc.) inevitably result in density variations which in turn affect the sputtering yields. Equation (1)[4] shows that the ion sputtering yield Y (atoms/ion) is proportional to the sputtering rate S (Å/min) and the density d(g/cm^3), and inversely proportional to the ion beam current density J (μA/cm^2) and atomic or molecular weight A (g):

$$Y = Sd/(0.06JA). \quad (1)$$

It is interesting to note that sputtering yield data roughly follow the number of electrons in the d shell and also show some similarity to the reciprocal of the heats of sublimation of the target materials.[5,6] The sputtering yield increases fairly linearly with ion beam energy above the threshold energy until it shoulders off and then saturates. For some materials the sputtering yield then decreases with increasing ion beam energy.[7]

The experimental parameters of the sputtering ion beam may also affect the sputtering rates. Some of these parameters are pertinent to the characteristics of the ion source used, such as spectral purity of the sputtering species (mass analyzed, neutrals, etc.), gas purity in the source region, ion beam energy, incident angle, gas pressure and composition in the analyzing chamber, current density, and shape. Doubly charged ions and neutrals which result from thermally excited ion sources if no mass separation is used have been observed to have different sputtering yields than their singly ionized counterparts.[8,9] The angle of incidence of the sputtering beam relative to the crystallographic orientation of the specimen also causes sputtering yield variations.[10] The

 0734-2101/88/032077-05$01.00 © 1988 American Vacuum Society

interface resolution between successive layers is a function of ion sputtering geometry[11] as well.

One must except localized sputtering rate variations for polycrystalline materials since their microcrystallographic planes may have different orientation to the sputtering beam. The crystallographic orientation is thought to be the major source of sample roughening from ion sputtering. One must also consider differences between directional ion sputtering sources such as "sputter ion guns" which are commonly used in Auger, electron spectroscopy for chemical analysis, and secondary ion mass spectroscopy instruments with "diffuse" plasma-type ion etchers. The orientation of single-crystal materials must be known before sputtering yield data can be determined or applied. Diffuse-type sputtering sources should leave smoother surfaces after sputtering. In the case of amorphous materials the choice of sputtering source should be less critical.

The ion beam current density, or dose, affects the surface temperature of the target material. At high current density the ion beam can anneal the target, changing the crystalline structure increasing the ion yield.[12] It can also increase the atomic vibrations about their mean positions in the locality of the damage event, reducing momentum transfer along collision chains, thereby reducing the sputtering yield.[13] Ion current densities of 5 mA/cm^2 cause target temperatures to rise 300–500 °C. One has to be mindful of the conditions under which the ion yields were originally determined in order to decide if they are being cogently applied. Ion beams can be stationary or rastered and yet have equivalent current densities, however, the instantaneous current density will differ. Uniformity of the beam may be better with a focused and rastered beam, as in our case.

One should also be aware of the techniques used to generate the sputtering ion yield data, once the sputtering conditions are known, to determine further their validity for the chosen application. Fine[14] has identified a variety of techniques used to measure ion sputtering yields. Measurements can be made on a continuous or intermittent basis and can result in either absolute or relative quantities. Fine has further classified the measurement techniques into the following categories: decrease of target mass of thickness, accumulation of sputtered particles as a thin film or in the gas phase, and finally, the interface detection method (such as the breakthrough method used in this work).

III. EXPERIMENTAL PROCEDURE

This article offers the results of sputtering yield measurements for a variety of sputtered thin films used in microelectronics. The resulting sputter yields were found to be repeatable within ~5% under the specific conditions which were used to make the measurements. These "low-dose" ion sputtering measurements were made using identical conditions to those under which "routine" specimens are analyzed in our laboratories. Since most of the specimens we depth profile consist of sputter deposited materials, it was prudent to prepare a set of similar materials in the same thickness range.

We decided to make the measurements on a static basis, using target thickness reduction combined with Auger interface detection. This allows us to make absolute determinations of the sputtering yield using Eq. (1), with experimentally determined S and J values in the Auger system and with d values obtained by Rutherford backscattering spectroscopy (RBS).

Thin films of Al, Al_2O_3 (containing 10% Ar), Au, Cr, Co, Cu, Fe, InSb, Sb, Ta, Ti, and $Ti_{0.12}W_{0.88}$ were sputter deposited onto a Cr seed layer, a thin thermally grown SiO_2 layer, or directly onto a polished [111] silicon wafer. Sputtering experiments were also performed using the National Bureau of Standards standard reference material (SRM #2135a) containing alternating Ni and Cr layers. Compositions of all the films were analyzed using both energy-dispersive x-ray and Auger spectrometers mounted on the instrument. The samples were cleaved into ~1-cm squares for the Auger microprobe analysis. Two different JEOL JAMP-10(S) scanning Auger microprobes were used to obtain data on each film. The agreement between data collected on the instruments was better than 5%. Each instrument's base pressure was below 1×10^{-9} Torr prior to ion sputtering. All measurements were made using a 10-keV stationary electron beam with 0.5-μA beam current, defocused over a 50-μm area (20 mA/cm^2) to minimize electron beam damage. The sample plane was perpendicular to the electron beam, with the ion gun at 55° to the sample axis normal. In the JAMP-10(S) microprobe, the cylindrical mirror analyzer (CMA) electron detector is positioned in such a way that its axis is in the sample plane.[15] Auger spectra were collected in the $E*dNE/dE$ mode. Both Auger instruments had scanning electron microscope (SEM) imaging capabilities.

Ion sputtering was accomplished with a Kratos Mini-Beam II differentially pumped ion gun. Prepurified argon gas was used in the ionizing chamber at a pressure of 1×10^{-3} Torr (gas saturation). The ion gun was differentially pumped using a turbomolecular pump. The sample chamber pressure was maintained at 5×10^{-8} Torr. The partial pressure of the sample chamber was monitored to insure that the sputtering gas and ion gun system introduced no significant level of contamination which would compromise

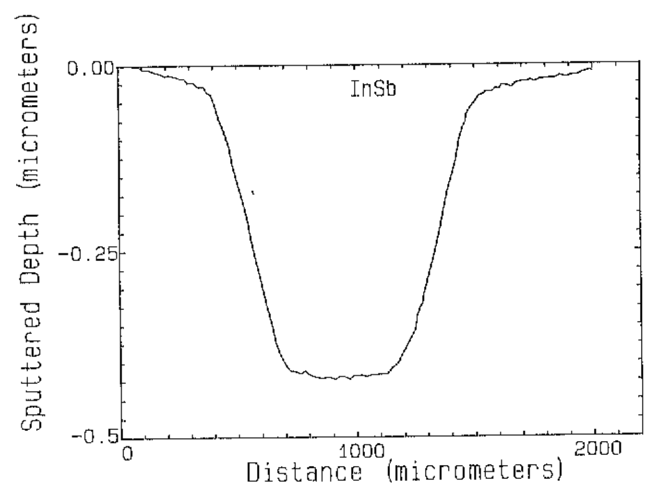

FIG. 1. Profilometer trace across the ion sputter crater of a 4.8-μm-thick InSb film at breakthrough. The flat bottomed crater illustrates uniformity of the ion sputtering beam (with rotation).

TABLE I. Thin-film sputtering yields using 1.5- and 3.0-kV Ar^+ beams.

Film	Measured thickness (Å)	Density RBS	Density Bulk (g/cm^3)	1.5 kV Yield (atom/ion)	1.5 kV Rate % SiO_2	3.0 kV Yield (atom/ion)	3.0 kV Rate % SiO_2
Al	4000	1.97	2.70	3.37	0.94	5.13	1.0
Si	4300	bulk	2.33	...	...	3.91	0.68
Ti	5400	4.39	4.50	2.13	0.47	3.40	0.53
Cr	3700	5.57	6.60	3.32	0.63	4.72	0.63
Fe	2100	5.25	7.83	3.24	0.71	4.50	0.68
Co	5800	6.11	8.71	3.05	0.60	3.32	0.47
Ni	2650	...	8.75	...	0.68	...	0.58
Cu	3200	5.91	8.89	4.53	1.22	9.53	1.47
Ta	3500	12.9	16.6	2.09	0.60	2.60	0.52
Au	6000	16.9	19.3	5.09	1.20	8.98	1.50
Ti–W (12–88)	1450	8.67	...	1.59[a]	0.64	...	...
Al_2O_3	3600	2.90	...	0.74[a]	0.53	1.08[a]	0.54
InSb	5700	5.48	...	...	...	3.93[a]	2.43

[a] Based upon molecules/ion.

the target surface purity. Ion beam energies of 1.5 and 3 kV were used to sputter the thin films with a 100-μm focused ion beam rastered over an area of 0.7 mm^2. Ion beam current densities were $\sim 4\ \mu A/cm^2$.

The intensities of the characteristic Auger peaks for the major elements of the analyzed film and that of the substrate were monitored through the depth of the film. The sputtering was terminated when the Auger electron intensity decreased to 50% of its maximum value (the breakthrough point). Reproducibility of the sputtering process was monitored by determining the sputtering rate of a standard 250-Å SiO_2 film before and after each experiment. The depths of the craters were then measured using a Tencor Alpha Step 200 surface profilometer. A typical crater profile is shown in Fig. 1, illustrating the flat-bottomed crater resulting from rastering the ion beam.

Since the density of a sputter-deposited material can be different from the bulk density, the density of each thin-film sample was determined independently by RBS (General Ionex model 4175 employing a 1-mm, 2-MeV He^{++} beam). The accuracy of this method relies upon the accuracies of the stopping cross sections as well as the measured thicknesses. Stopping powers are known to be within 5%–10%, imposing a fundamental accuracy limitation.

IV. RESULTS

Following this experimental procedure measurements were made on the films listed in Table I. The table summarizes the sputtering yields at 1.5 and 3 kV along with the films' thicknesses, densities, and the sputtering rates relative to that of SiO_2. This last term shows the relative rate at which each film sputters. If the sputtering rates were known for all the components analyzed in a real sample, the depth profile could be plotted with an absolute depth scale. The usefulness of relative sputtering rates is limited since the densities of the films must be known.

Sputtering rates measured on several of the films with the same compositions and densities, but with different thicknesses, varied significantly. SEM image observations of these films craters indicated that the ion sputtering process resulted in surface roughening. This is a usual occurrence when sputtering polycrystalline materials.

After several hours of ion sputtering we were unable to completely remove the 5725-Å InSb film. In and Sb do sputter at different rates, however, as one element is preferentially sputtered its surface concentration decreases and an equilibrium is quickly reached. Since the ion sputtering yield is a function of the orientation of the microcrystalline grains of the material one would expect surface roughening to occur. A possible mechanism which may account for the incomplete sputtering of the InSb film is a high degree of redeposition of the sputtered atoms within the film such that few atoms actually leave the film. An example of this roughening is illustrated in Fig. 2.

In order to confirm this assumption, the measurements on some films were performed in an incremental manner. After the breakthrough time was determined for the Ti, Co, and Cr

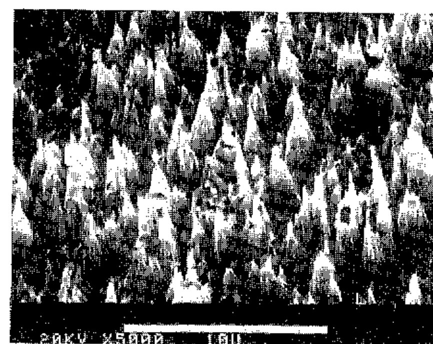

FIG. 2. SEM photomicrograph illustrating the topographic directionality induced by ion sputtering, without rotation, on an InSb film deposited on smooth GaAs at breakthrough.

films, "fresh" areas were sputtered in fractional time increments in order to determine whether the depth of the craters obtained was directly proportional to the sputtering time. Figure 3 presents the incremental sputtering rates for these three films. The incremental rate represents the amount of material removed between the successive time increments divided by the corresponding time interval. The plots clearly indicate that the incremental sputtering rate decreases with depth. The largest decrease in sputtering rate for both Ti and Cr was 39% and 37%, respectively, which represents the time increment for sputtering 75% of the full breakthrough time. The titanium film showed no decrease in the sputtering rate until $\frac{1}{2}$ to $\frac{3}{4}$ of the full sputtering time for the 5400-Å film. The Cr film showed the decrease much sooner, within the $\frac{1}{4}$ to $\frac{1}{2}$ time range of the full film thickness.

Two possible causes are considered to explain this effect. The profilometer's large stylus's radius (25 μm) in comparison with the microtopographic surface roughness (0.02 μm) may result in the stylus riding on the high points of the film surface, thereby contributing to nonlinearity of the measurements results. However, the magnitude of this error is much smaller than the sputtering rate loss. Another possible cause (but one which we doubt) may be density variations throughout the depth of the film.

A similar phenomenon (but to a much lesser degree) was observed on the NBS SRM #2135a nine-layer alternating Ni/Cr film. Measurements of the sputtering time to the midpoint (50% Cr and 50% Ni concentration) between each layer for the 530-Å Cr film and the 640-Å Ni film in both our data and those from NBS indicated a slight progressive decrease in the sputtering rate as a function of depth.

The sputtering rate decrease for the total thickness of the Cr–Ni NBS SRM is significantly less than that of the Ti, Co, and Cr films we measured. As the film composition changes from Cr to Ni and back again, both the crystallographic orientation and composition change preventing the formation of sputter induced roughness. If we assume that this slight decrease in the ion sputtering rate corresponds to the roughening of the surface caused by microchannelling effects of the polycrystalline surface,[16] we can understand why more topographic roughening is observed on the thicker films of uniform composition.

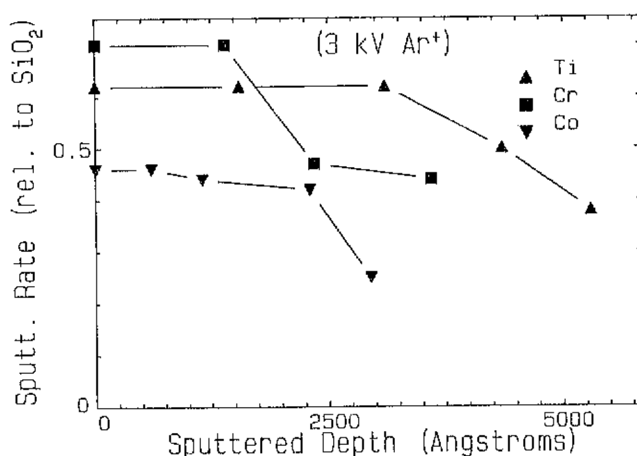

FIG. 3. Sputtering rate loss for Co, Ti, and Cr with increasing sputtered depth. The rate, relative to SiO_2, is the rate between successive thicknesses of material removed.

The microchanneling effect of the thicker films and the resulting sputtering rate decrease produced by the ion sputtering process adds thickness of the analyzed material as another limitation to the general applicability of ion sputtering yield tables.

Table I illustrates that the sputtering yields and sputtering rates are different quantities which are related by the density and mass of the sputtered material. A larger sputtering yield for a material does not necessarily mean a higher sputtering rate (see, for instance, Co and Ta). The advantage in using the relative sputtering rates' values (based upon that of SiO_2) is in providing a convenient basis for comparison of the actual removal rates, assuming that films of the same composition have the same density.

V. SAMPLE ROTATION DURING SPUTTERING

It has been suggested by some authors[17,18] and demonstrated by Zalar[16] that surface topography effects can be reduced by azimuthally rotating the specimen while it is being sputtered. Unfortunately, the instability of Zalar's stage rotation mechanism caused changes in the specimen's position with respect to the CMA's focal point, thereby increasing the measurement noise. With continuous stage rotation (at 0.5 rpm) in our instrument, no statistically significant noise was detected above the normal level. Using SEM imaging, we found no evidence of topographical roughening after sputtering through the Ti and Cr films using sample rotation. The incremental sputtering rates measured on these films with rotation were found to be uniform throughout the thickness of the films.

The InSb film, which was previously described as being difficult to analyze, was sputtered, with rotation, completely down to the substrate within a reasonable length of time. There was no obvious topographic directionality in the film at the breakthrough depth.

The analysis of the NBS SRM #2135a with stage rotation during sputtering indicated that the time required to sputter through each Cr and Ni layer did not change with depth and the interface widths from layer to layer were constant. Zalar noted the same result on a similar specimen. Figure 4 confirms his findings comparing depth profiles of this material with and without rotation using a 3-kV Ar^+ ion beam.

VI. CONCLUSION

Quantification of the ion sputtering process is limited by a number of factors related to the materials analyzed and the analysis techniques. Recognizing these limitations, the general use of the sputtering yields tables requires the following: (1) The measurements should be performed on materials with known densities; (2) reference materials and the experimental materials should have similar compositions, crystallinity, orientation, and surface characteristics; (3) ion sputtering geometry, energy, dose, gas species, residual gas vacuum levels and gas purity characteristics should be similar; and (4) the measurement techniques to determine the amount of removed material should be identical to those used for the reference data.

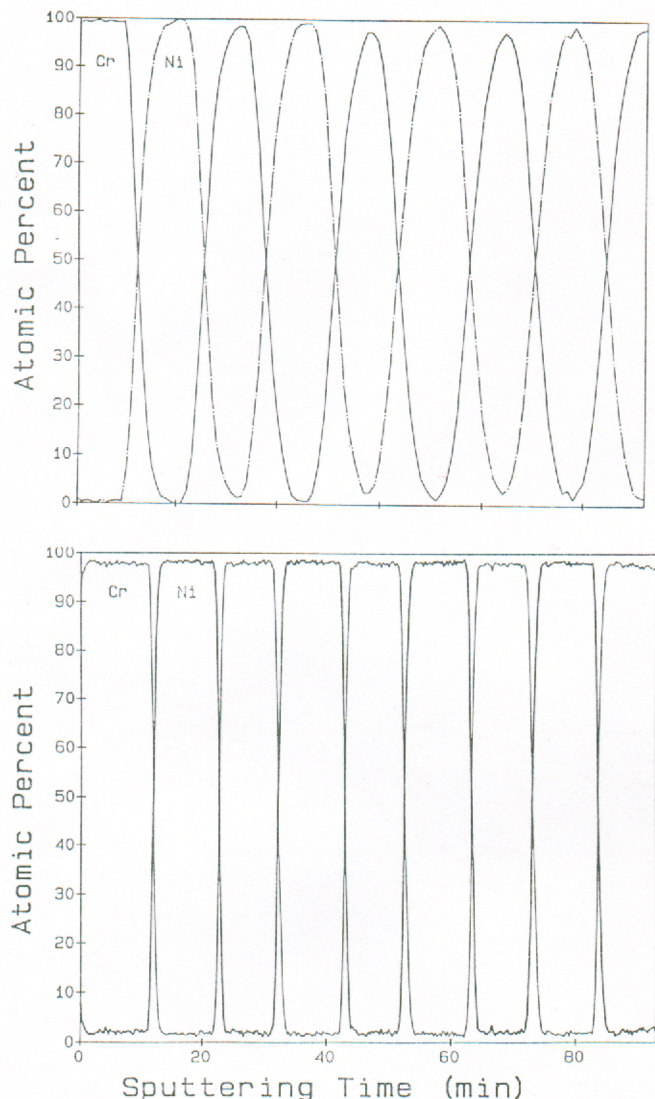

FIG. 4. Depth profiles of NBS #2135a, Cr(53 nm)/Ni(64 nm) multilayer film. The data were collected with the specimen stationary (upper) and rotating (lower) during ion beam sputtering. Rotating the specimen preserves depth resolution throughout the thickness of the film.

Absolute sputtering rates can be measured on easily available thin films of known thicknesses of SiO_2 on Si. Using the ion sputtering rate (as opposed to the yield) gives one a direct measure of the relative speed at which one material sputters with respect to another, as long as the densities of each material are known. Finally, sample rotation during ion sputtering is an effective way to reduce surface roughening of the sputtered material. As has been demonstrated in some specific cases, sputtering rates and yields which had previously been seen to decrease with sputtered thickness have remained constant. Sample rotation during sputtering is also an effective way to preserve depth resolution. This should have some impact upon the theoretical calculations and assumptions used to describe the ion sputtering process.

ACKNOWLEDGMENTS

The authors would like to express their thanks to Kelly Wollenberg for help in performing profilometer measurements and to Peter Revesz of General Ionex for the RBS measurements. The authors also wish to express their appreciation to Dr. J. Fine from NBS for invaluable discussions on the subjects of this article.

[1]S. Hofmann, Surf. Interface Anal. **2**, 4 (1980).
[2]*Sputtering by Particle Bombardment I*, edited by R. Behrisch (Springer, New York, 1981), Vol. 47, Chap. 4.
[3]*Ion Bombardment of Solids*, edited by G. Carter and J. S. Colligon (American Elsevier, New York, 1968), pp. 323–325.
[4]*Methods of Surface Analysis*, edited by A. W. Czanderna (Elsevier, New York, 1975), p. 14.
[5]N. Laegrid and G. K. Wehner, J. Appl. Phys. **32**, 365 (1961).
[6]D. Rosenberg and G. K. Wehner, J. Appl. Phys. **33**, 1842 (1962).
[7]In Ref. 3, p. 314.
[8]S. P. Wolsky and E. J. Zdanuck, Phys. Rev. **121**, 374 (1961).
[9]A. Weiss, A. Heldt, and W. J. Moore, J. Chem. Phys. **29**, 7 (1958).
[10]In Ref. 4, p. 12.
[11]K. Wittmaack, J. Vac. Sci. Technol. A **4**, 1662 (1986).
[12]In Ref. 3, p. 334.
[13]T. W. Snouse and M. Bader, in *Transactions of the 8th National Vacuum Symposium* (Pergamon, New York, 1962), Vol. 1, p. 271.
[14]J. Fine, in *The Physics of Ionized Gases*, edited by M. Matic (Boris Kidric Institute of Nuclear Sciences, Beograd, 1980).
[15]J. D. Geller, Appl. Surf. Sci. **18**, 18 (1984).
[16]A. Zalar, Thin Solid Films **124**, 223 (1985).
[17]D. E. Sykes, D. D. Hall, R. E. Thompkins, and J. M. Walls, Appl. Surf. Sci. **5**, 103 (1980).
[18]P. H. Holloway and R. S. Baftacharya, Surf. Interface Anal. **3**, 3 (1981).